High-resolution atmospheric angular momentum functions related to Earth rotation parameters during CONT08

Michael Schindelegger Johannes Böhm David Salstein Harald Schuh

M. Schindelegger, J. Boehm, H. Schuh:
Institute of Geodesy and Geophysics, Vienna University of Technology
Gußhausstraße 27-29, 1040 Vienna, Austria
michael.schindelegger@tuwien.ac.at

D. Salstein:
Atmospheric and Environmental Research, Lexington, U.S.A

Abstract

Due to the temporal resolution of available numerical weather analyses, the effect of the atmosphere on Earth rotation at daily and sub-daily periods is usually investigated by using six-hourly atmospheric angular momentum (AAM) functions. During the period of CONT08, however, atmospheric analysis data were provided by the European Centre for Medium-Range Weather Forecasts (ECMWF) also on an hourly basis. In this paper, we therefore determine two sets of AAM functions from ECMWF data - one for CONT08 with hourly resolution and one for the year 2008 with six-hourly resolution. The comparisons of the AAM functions to high-resolution Earth Rotation Parameters (ERP) from VLBI and GPS observations are carried out in the frequency domain. Special attention is paid to the preparation of the high-resolution data sets for the geodetic purposes, as there are jump discontinuities at 12 hour intervals. Hence, the hourly AAM functions need to be concatenated. The revised functions yield much smaller amplitudes than their six-

hourly counterparts, as can be seen from the equatorial and the axial frequency spectra of atmospheric excitation in Earth rotation. This decrease of spectral power in the hourly AAM functions is found to be associated with a strong counteraction of pressure and wind terms, which originates from atmospheric circulation on short time scales. The results are compared to previous findings published by Brzeziński and Petrov (2000) based on data from the U.S. National Centers for Environmental Prediction (NCEP).

Keywords

Earth rotation, atmospheric angular momentum, high-frequency excitation of Earth rotation

1 Introduction

The angular momentum of the atmosphere, one of the fluid portions of the Earth, shows significant temporal variations, caused by large-scale mass redistributions and changes in wind patterns. In the absence of external torques, the angular momentum of the system consisting of the solid Earth plus its fluid layers must be conserved, or, in other words, changes of the angular momenta of the solid Earth and the fluids (the atmosphere, for instance) are of equal size but otherwise opposite. Changes in the angular momentum of the solid parts of the Earth, however, are manifested in fluctuations of the rotation of our planet. In this way, large-scale atmospheric processes contribute to all components of Earth rotation: polar motion, nutation and changes in length of day (LOD).

A formal description of the dynamic relation between atmosphere and solid Earth was initially derived by Munk and MacDonald (1960) based on linearizing the equations of motion of a non-rigid rotating body. The excitation functions, central to this linear theory, have since been reformulated and modified by several authors, e.g. Wahr (1982), Barnes et al. (1983) or Eubanks (1993). Barnes et al. (1983) suggested replacing the original excitation functions by the effective atmospheric angular momentum (AAM) functions, which can be particularly well calculated from globally gridded meteorological data. The equation relating atmospheric or any fluid excitation to the equatorial part of Earth rotation was extended for the Free Core Nutation (FCN) resonance (Sasao and Wahr, 1981) by

Brzeziński (1994), allowing the investigation of atmospheric effects in polar motion and nutation on all time scales. For periods of a few days or longer, observed Earth rotation variations and those estimated from AAM functions are in good agreement, e.g. Barnes et al. (1983) or Salstein et al. (1993). At diurnal and semi-diurnal frequencies, however, the value of coherence between AAM functions and geodetic observations is significantly lower, as ocean tidal effects are much more dominant on these short time scales, both for variations in Earth's rotation rate (Ray et al., 1994) and for polar motion (Chao et al., 1996). Nonetheless, Zharov (1994) or Brzeziński and Petrov (2000) estimate amplitude and phase for the high-frequency atmospheric signals in Earth rotation, which appear to be predominantly tidal waves of thermal origin that cause sharp peaks at $T = \pm 12, \pm 24$ h in the excitation spectra. Bizouard et al. (1998), Brzeziński et al. (2002) or Vondrák and Ron (2007) highlight the considerable contribution of atmospheric tides to nutation, demonstrating that geophysical excitation in this frequency band is largely amplified by the presence of the FCN resonance, see the assertions of earlier theoretical studies (Sasao and Wahr, 1981; Brzeziński, 1994). Diurnal and semi-diurnal atmospheric effects on Earth Rotation Parameters (ERP), polar motion and changes in LOD, are below 10 μas or 10 μs, respectively, and thus by one order of magnitude smaller than the atmospheric forcing of nutation amplitudes (Brzeziński et al. 2002). Considering the prospective measurement accuracies of space geodetic techniques, however, high-frequency atmospheric excitations of ERP are non-negligible.

The main purpose of this work is to determine and compare diurnal and semi-diurnal excitation signals in polar motion and LOD from different meteorological data classes of the European Centre for Medium-Range Weather Forecasts (ECMWF). Standard six-hourly AAM functions are estimated for the year 2008 based on the ECMWF operational analysis data, whereas hourly AAM functions are derived from the ECMWF 4DVar analysis for the time span of the CONT08 measurement campaign, which is described in the next paragraph. In principle, both AAM series can be processed similarly. The hourly functions series, though, have clear discontinuities at 9 and 21 UTC, which are the initialization epochs for the 12-hourly update of the forecast model used within the 4DVar algorithm. This particular feature restrains calculations in the frequency domain and it is thus imperative to remove such jumps from the original AAM functions (see Section 3).

CONT08, scheduled from August 12 to August 26, 2008, provided two weeks of continuous Very Long Baseline Interferometry (VLBI) observations and extended the series of the special CONT campaigns, which all demonstrated the highest possible quality of contemporary VLBI data (1994, 1995, 1996, 2002 and 2005). Among other scientific and technical goals, CONT08, as well as CONT02 and CONT05, was designed to support studies of daily and sub-daily variations in Earth rotation, see e.g. Haas and Wünsch (2006) or Artz et al. (2010). The atmospheric excitation of high-frequency ERP signals was expected to be large during the time of the northern hemisphere summer, and it is therefore interesting to ask for the atmospheric contribution to diurnal and semi-diurnal polar motion and LOD from CONT08 after removal of the ocean tidal effects.

Our study addresses the latter question by estimating the excitation amplitudes in ERP from hourly AAM series during CONT08. Although the limited length of this dataset does not allow a fine resolution of the spectral structure at $T = \pm 12$ h and $+24$ h, mean amplitudes can be obtained for each tidal band and may confirm the results derived from six-hourly AAM functions. These mean amplitudes are of particular interest for the semidiurnal band, where a clear distinction between pro- and retrograde contributions is only feasible for the hourly AAM series. Throughout this work, the amplitude estimates from atmospheric data are compared with geodetic ERP, which are hourly polar motion and LOD from Global Positioning System (GPS) data and VLBI observations acquired during CONT08.

2 Atmospheric angular momentum functions and Earth rotation

The angular momentum of the atmosphere $\mathbf{H}^{(a)}$ is a three-dimensional quantity and it can be split up into two components, usually referred to as matter and motion terms (or pressure and wind terms). The matter term describes the influence of atmospheric mass redistributions on the Earth's inertia tensor $\mathbf{I}$, resulting in time-dependent perturbations ΔI_{ij} $(i, j = 1, 2, 3)$, of which only the components ΔI_{i3} $(i = 1, 2, 3)$ are connected with changes in Earth rotation. The motion term corresponds to the relative angular momentum $\mathbf{h}$ of the atmosphere with respect to the mean rotating reference system. In its most

practical formulation, e.g. given by Moritz and Mueller (1987), $\mathbf{H}^{(a)}$ is estimated from surface pressure data p_s and from the global fields of zonal and meridional wind velocities u and v:

$$\mathbf{H}^{(a)} = \Omega\Delta\mathbf{I} + \mathbf{h} = \Omega \begin{pmatrix} \Delta I_{13} \\ \Delta I_{23} \\ \Delta I_{33} \end{pmatrix} + \begin{pmatrix} h_1 \\ h_2 \\ h_3 \end{pmatrix} , \tag{1}$$

$$\Delta\mathbf{I} = -\frac{R^4}{g} \int_0^{2\pi} \int_{-\pi}^{\pi} p_s \cos^2\phi \begin{pmatrix} \sin\phi\cos\lambda \\ \sin\phi\sin\lambda \\ -\cos\phi \end{pmatrix} d\phi\, d\lambda \, , \tag{2}$$

$$\mathbf{h} = -\frac{R^3}{g} \int_0^{2\pi} \int_{-\pi}^{\pi} \int_0^{p_s} \cos\phi \begin{pmatrix} u\sin\phi\cos\lambda - v\sin\lambda \\ u\sin\phi\sin\lambda + v\cos\lambda \\ -u\cos\phi \end{pmatrix} dp\, d\phi\, d\lambda \, . \tag{3}$$

Here, ϕ and λ denote latitude and longitude, dp is the positive pressure increment for vertical integration, R is the Earth's mean radius, g is the mean acceleration due to gravity, and Ω is the Earth's mean angular velocity. To determine the rotational perturbations of the Earth induced by the atmosphere, dimensionless effective AAM functions have to be deduced from Equation (1). Maintaining the distinction between pressure (superscript p) and wind terms (superscript w), the AAM functions are further split up into equatorial and axial components $\hat{\boldsymbol{\chi}} = \chi_1 + \mathrm{i}\chi_2$ and χ_3

$$\hat{\boldsymbol{\chi}} = \frac{1.057\,\Omega\Delta\hat{\mathbf{I}} + 1.394\,\hat{\mathbf{h}}}{(C - A')\Omega} = \hat{\boldsymbol{\chi}}^p + \hat{\boldsymbol{\chi}}^w, \tag{4}$$

$$\chi_3 = \frac{0.757\,\Omega\Delta I_{33} + 0.999\,h_3}{\Omega C_m} = \chi_3^p + \chi_3^w, \tag{5}$$

where the complex quantities stand for $\Delta\hat{\mathbf{I}} = \Delta I_{13} + \mathrm{i}\Delta I_{23}$ and $\hat{\mathbf{h}} = h_1 + \mathrm{i}h_2$, respectively. A' and C are the mean equatorial and polar moments of inertia of the whole Earth and C_m denotes the polar moment of inertia of the mantle. Numerical values for geodetic parameters are taken from Gross (2007). The factors leading pressure and wind terms in (4) and (5) account for the responses of Earth's different portions to the rotational fluctuations evoked by an initial excitation. However, our scaling factors differ somewhat from those of other authors, see for example the original transfer coefficients of Munk and MacDonald (1960) or the recent estimates in Gross (2007). This deviation can be ex-

plained by our approach of basically employing the equations of Dickman (2005) designed to consistently incorporate core-mantle interactions in the excitation formalism. In detail, the system of differential equations, describing the rotational perturbations caused by any fluid, is phrased for the whole Earth in order to reflect the essential assumption of angular momentum balance within the Earth-fluid system. The pivotal modification made to the system is the introduction of a core which is decoupled from the mantle. As indicated in earlier excitation studies, e.g. Brzeziński (2002), this assumption is justified since the liquid outer parts of the core cannot follow rotational fluctuations of the mantle on time scales of several days or smaller. Equations (2) and (4) of Dickman (2005) are adopted to relate excitation (or AAM) functions $\hat{\boldsymbol{\chi}}$, χ_3 to LOD and polar motion variations and simultaneously allow for a fully decoupled core. The absent coupling between core and mantle affects Earth's inertia, even though it does not reduce $C - A'$ in the denominator of Equation (4) to the corresponding mantle-only value (Dickman, 2003). The load and rotational Love numbers, though, are required to be phrased for the mantle. In particular, this implies to downscale the rotational Love number $k2 = 0.30097$ of an oceanless Earth at high frequencies according to Dickman, 2005. Generally speaking, the obtained equations describe the reaction of an anelastic Earth with a fluid core to changes in the centrifugal and loading potential. Mass redistributions in the oceans, which would also arise from rotational variations and subsequent perturbing centrifugal forces, cannot be considered here due to the lack of a model for this effect at daily and sub-daily time scales.

Comparison of the AAM functions $\hat{\boldsymbol{\chi}}$ and χ_3 with ERP, which are polar motion $\hat{\mathbf{p}} = x - \mathrm{i}y$ of the Celestial Intermediate Pole (CIP) and LOD, is only straightforward for the axial component

$$\chi_3 = \mathrm{LOD} + \mathrm{const}, \tag{6}$$

whereas the equatorial case involves transfer functions considering two eigenmodes of the Earth, the Chandler Wobble (CW) and the Nearly Diurnal Free Wobble (NDFW), or its celestial counterpart, the FCN. On the basis of the theoretical work of Sasao and Wahr (1981), Brzeziński (1994) arrived at the following relationship in the frequency domain:

$$\hat{\mathbf{p}}(\sigma) = \hat{\mathbf{T}}_p(\sigma)\hat{\boldsymbol{\chi}}^p(\sigma) + \hat{\mathbf{T}}_w(\sigma)\hat{\boldsymbol{\chi}}^w(\sigma). \tag{7}$$

$\hat{\mathbf{T}}_p(\sigma)$ and $\hat{\mathbf{T}}_w(\sigma)$ are the transfer functions for pressure and wind terms of the AAM functions, comprising $a_p = 9.2 \cdot 10^{-2}$ and $a_w = 5.5 \cdot 10^{-4}$ as specific constants:

$$\hat{\mathbf{T}}_p(\sigma) = \hat{\boldsymbol{\sigma}}_{cw} \left(\frac{1}{\hat{\boldsymbol{\sigma}}_{cw} - \sigma} + \frac{a_p}{\hat{\boldsymbol{\sigma}}_f - \sigma} \right), \tag{8}$$

$$\hat{\mathbf{T}}_w(\sigma) = \hat{\boldsymbol{\sigma}}_{cw} \left(\frac{1}{\hat{\boldsymbol{\sigma}}_{cw} - \sigma} + \frac{a_w}{\hat{\boldsymbol{\sigma}}_f - \sigma} \right). \tag{9}$$

Adopting the numerical values suggested by Eubanks (1993), the complex eigenfrequency for the CW is

$$\hat{\boldsymbol{\sigma}}_{cw} = \frac{2\pi}{T_{cw}} \left(1 + \frac{\mathrm{i}}{2Q_{cw}} \right), \tag{10}$$

with $T_{cw} = 433$ d and $Q_{cw} = 179$, though estimates for the quality factor Q_{cw} have varied considerably. The eigenfrequency of the NDFW is derived analogously from T'_f, the period of the FCN in the celestial frame, and Q_f, its Earth-referred quality factor. Both values are taken from the conventional precession-nutation model (Mathews et al., 2002):

$$\hat{\boldsymbol{\sigma}}_f = 2\pi \left(\frac{1}{T'_f} - \frac{1}{T_{sid}} \right) \left(1 - \frac{\mathrm{i}}{2Q_f} \right). \tag{11}$$

The numerical values are $T'_f = -430.2$ d, $Q_f = 20000$ and $T_{sid} = 0.9973$ d, describing the length of the sidereal day. Evaluation of Equation (11) yields a frequency of resonance at $\sigma = -1.00232$ cycles per sidereal day (cpsd), located in the nutation band, which comprises motion of the CIP in the frequency range of $\sigma = [-1.5, -0.5]$ cpsd if viewed from the terrestrial frame. Considering the FCN resonance is therefore indispensable when studying atmospheric forcing of nutation (Bizouard et al., 1998 or Brzeziński et al., 2002). As for polar motion, the influence of the FCN is small, but non-negligible at least for the pressure term (Equation 8), see Brzeziński (1994) for further details.

3 Concatenation of AAM functions from forecast data

3.1 The 4DVar analysis

In contrast to the conventional six-hourly AAM functions that are estimated from operational analysis data, hourly AAM functions can only be determined from the ECMWF system based on a 4DVar analysis (Four-dimensional Variational Assimilation, see Perrson and Grazzini, 2007). The idea of a 4DVar analysis is similar to that of a Kalman filter:

initialized at 9 and 21 UTC, every 12 hours the most recent observations are assimilated in order to update an atmospheric forecast model in an integration (Figure 1). Evaluation of the updated model trajectory every single hour yields high-resolution meteorological analysis fields.

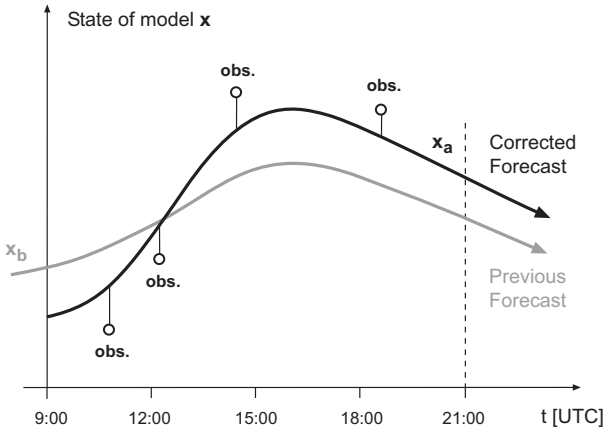

Figure 1: Illustration of the 4DVar principle: Updating a forecast model by including observations.

3.2 Concatenation of hourly AAM functions

Due to the interval-wise application of the 4DVar analysis, hourly AAM functions are generally available as 12 hour-arcs, separated by jump discontinuities at the interval borders, which are at 9 and 21 UTC. In order to properly estimate amplitude spectra of atmospheric excitation, these jumps have to be removed from the time series. Two methods of concatenating the arcs in AAM functions are employed:

Variant 1 (see Figure 2): The offset $\overline{y}$ at 9 or 21 UTC is distributed to the preceding 12 hour-interval, so that each value with distance Δt from the jump discontinuity is corrected by

$$\left(\frac{\Delta t + 12}{12}\right)^{1.5} \overline{y}\,.$$

To smooth the resulting function, we define cubic polynomials, which replace the original values in the neighborhood of the remaining slope discontinuities. The interval treated is chosen to stretch from $\Delta t = -5$ h to $\Delta t = 0$ h.

Variant 2 (see Figure 3): Translation of the 12 hour-arcs along the ordinate axis eliminates

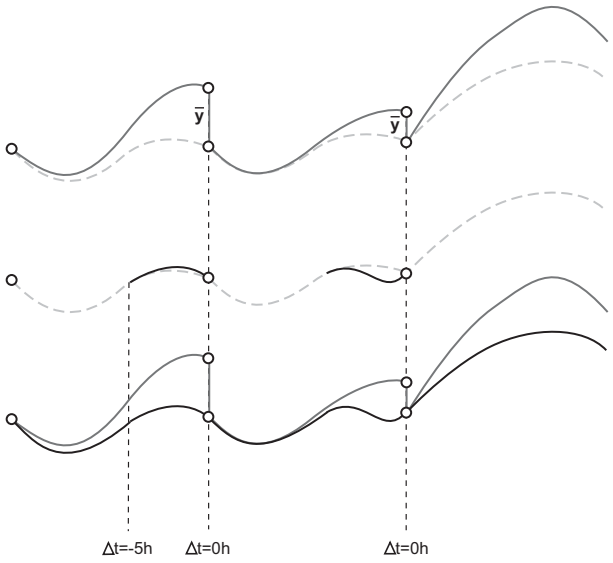

Figure 2: Concatenation steps for variant 1 (top-down). Upper part: distribution of $\overline{y}$ over the preceding interval. Middle part: smoothing of further discontinuities. Lower part: comparison of concatenated arcs (black line) and initial function (grey line).

the jumps of the initial AAM function f_0 and, similar to variant 1, cubic polynomials between $\Delta t = -2$ h and $\Delta t = 2$ h remove slope discontinuities at 9 and 21 UTC. This leads to the function f_1, of which the final value differs from that of the original function by $\overline{Y}$. Thus, $\overline{Y}$ is distributed linearly in time to f_1 over the whole time span, yielding f_2. Further adjustment is achieved, if a low-order Fourier series is calculated from the differences $\overline{y}$ between f_0 and f_2 at 9 and 21 UTC. Subtraction of this Fourier series from f_2 finalizes the concatenation.

The hourly AAM functions, which are determined from Equations (2) to (5) for a slightly larger time window (August 8 to August 31, 2008) than CONT08 (August 12 to August 26, 2008), are modified with both variants. Together with the six-hourly AAM functions, these are the time series used for comparison with ERP in the following sections.

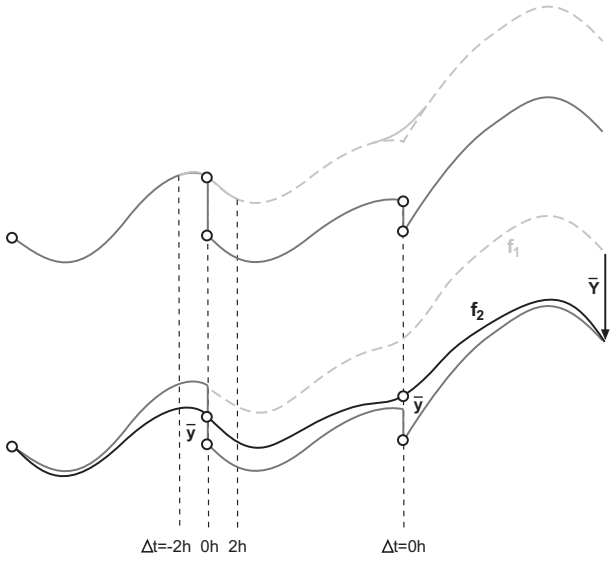

Figure 3: Concatenation steps for variant 2 (top-down). Upper part: Translation and smoothing of the arcs give f_1. Lower part: linear distribution of $\overline{Y}$. Subtraction of the Fourier series is not depicted.

4 Atmospheric excitation of polar motion and LOD from six-hourly AAM functions

The period of time investigated is the year 2008. In order to reach correspondence with AAM functions, which are available at 0, 6, 12 and 18 h UTC, the hourly record of ERP from GPS (reprocessed CODE series, Bernese software, see Steigenberger et al., 2006) has to be sampled at the same epochs. Since the main part of variations in Earth rotation at high frequencies is due to ocean tides, we remove this influence on the geodetic series by applying the IERS Conventions model (McCarthy and Petit, 2004), which is based on Ray et al. (1994). The residual amplitude spectra of polar motion and LOD at daily and sub-daily periods are shown in Figures 4 and 5. The retrograde limit of Figure 4 is $T = -16$ h and practically coincides with the upper cut-off frequency of $\sigma = -1.5$ cpsd in nutation. However, as already stated, our study shall not particularly cover the nutation band, but merely concentrates on polar motion, so that the limits of Figure 4 are used for all equatorial plots in this paper. Moreover, the GPS series do not comprise retrograde

diurnal signals due to a specific constraint in its data processing.

Note that the geodetic spectra still contain residual ocean tidal effects which were not removed by the model recommended in the IERS Conventions. Assuming a tidal wave with an amplitude of some 200 μas with a model uncertainty of 5 to 10 %, the remaining oceanic effect in the spectrum could be as high as 10 to 20 μas at the specific tidal period.

The amplitudes in Figures 4 and 5 that can be assigned to variations of atmospheric angular momentum are estimated following the theoretical findings of Section 2. As for the axial component, the complex Fourier transforms of mass and motion terms can be added directly, so that

$$\chi_3(\sigma) = \chi_3^p(\sigma) + \chi_3^w(\sigma) = \mathrm{LOD}(\sigma) \tag{12}$$

holds in the frequency domain. For the equatorial AAM function, the distinction between mass and motion terms has to be maintained until $\hat{\boldsymbol{\chi}}^p(\sigma)$ and $\hat{\boldsymbol{\chi}}^w(\sigma)$ are multiplied with the complex transfer functions $\hat{\mathbf{T}}_p(\sigma)$ and $\hat{\mathbf{T}}_w(\sigma)$. If in Equation (7) $\hat{\mathbf{p}}(\sigma) = \hat{\mathbf{p}}_{\boldsymbol{a}}(\sigma)$ denotes the Fourier transform of polar motion due to atmospheric excitation, its amplitude spectrum is determined from the complex modulus $|\hat{\mathbf{p}}_{\boldsymbol{a}}|$.

The mean amplitudes at diurnal and semi-diurnal frequencies, both for the equatorial as well as the axial component, are summarized in Table 1. Comparative values for all frequency bands, taken from Brzeziński and Petrov (2000), are of similar size. The main differences stem from the fact that Brzeziński and Petrov (2000) use 40 years of reanalysis data and employ a more sophisticated spectral analysis compared to that which is done here. In general, atmospheric effects from six-hourly meteorological data are smaller than 10 μas or 10 μs in polar motion and LOD, respectively, and thus explain only about 25 % of the observed residual ERP variatons.

Diurnal retrograde signals in $\hat{\mathbf{p}}_{\boldsymbol{a}}(\sigma)$ are a by-product of our calculations and included in Table 1, for completeness. Since the AAM datasets of this study, especially the hourly series investigated in Section 5, are of a very limited length, the specific tides in the nutation band cannot be distinguished and it is only possible to give the amplitude of the broad peaks which are present at $T = -1.0$ d and $T = -1.2$ d.

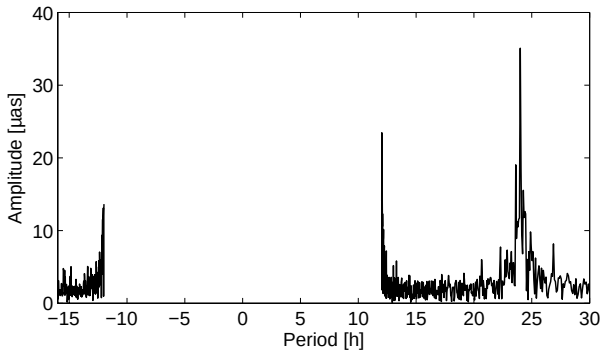

Figure 4: Amplitude spectrum of polar motion at diurnal and semi-diurnal periods, calculated from six-hourly GPS observations for 2008. Ocean tidal effects have been removed by applying the IERS Conventions model (McCarthy and Petit, 2004).

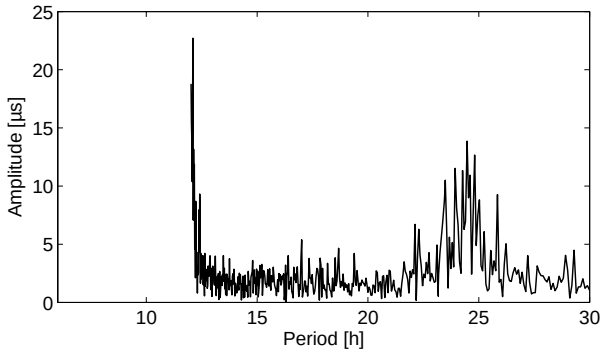

Figure 5: Amplitude spectrum of LOD at diurnal and semi-diurnal periods, calculated from six-hourly GPS observations for 2008. Ocean tidal effects have been removed by applying the IERS Conventions model (McCarthy and Petit, 2004).

Table 1: Atmospheric excitation: mean amplitudes of polar motion [μas], nutation [μas] and LOD [μs] at diurnal and semi-diurnal terrestrial periods, calculated from different meteorological records and compared to results obtained by Brzeziński and Petrov (2000) from NCEP reanalysis data (second data line).

	Polar Motion			Nutation		LOD	
Period (d)	1.0	0.5	-0.5	-1.0	-1.2	1.0	0.5
ECMWF, 6h, 2008 (this study)	**5.6**	**1.7**	**1.7**	**107**	**13**	**6.8**	**8.4**
NCEP, 6h, 40 years (Brzeziński & Petrov, 2000)	**7.0**	**2.9**	**2.9**	**183**	**30**	**6.0**	**3.3**
ECMWF, 6h, CONT08 (this study)	7.2	2.6	2.6	102	25	5.1	5.3
ECMWF, 1h, CONT08 (this study), concatenation 1	**2.6**	**0.9**	**1.0**	**59**	**9**	**1.3**	**1.3**
ECMWF, 1h, CONT08, without concatenation (this study)	1.4	1.1	2.6	61	9	2.6	1.5

5 Atmospheric excitation of polar motion and LOD from hourly AAM functions

For the geodetic series, we gather three different sets of high-resolution Earth rotation data for CONT08:

- The CODE GPS solution already used in Section 4.
- The VLBI solution estimated with Calc/Solve (Gordon et al., 2006).
- The VLBI solution determined with VieVS (Vienna VLBI Software, Böhm et al., 2009).

For the reasons given in the previous section, the equatorial spectrum is again not extended to the nutation band (retrograde diurnal motions are also not allowed in the VLBI series). The final plots of polar motion and LOD from the three ERP records are presented in Figures 6 and 7. Apparently, the two VLBI solutions agree very well, whereas the GPS solution gives different amplitudes especially for $T = \pm 12$ h in polar motion.

Considering the scale of the effects in the geodetic spectra and recalling the results of Section 4, we note that the atmosphere accounts only for a minor part of high-frequency ERP variability. By employing Equations (7) and (12) on the hourly AAM functions, the corresponding amplitude spectra (Figures 8 and 9) are obtained. For the first variant of concatenation, the mean amplitudes of the main peaks are listed in Table 1. Strikingly, we attain no agreement with the results of Section 4. Throughout, diurnal and semi-diurnal signals in polar motion and LOD from hourly AAM functions are about two times (or in the axial case up to six times) smaller than their six-hourly counterparts. These discrepancies cannot be ascribed to the fact, that hourly and six-hourly amplitude estimates are computed over different time spans, as even the six-hourly estimates just for the period of CONT08 (third data line in Table 1) do not containg the low magnitude prevailing for the hourly series. A second source for the observed differences could be the numerical procedures employed for concatenating the AAM series from 4DVar data. For that reason, it might be useful to determine the excitation amplitudes from the original hourly AAM functions. It has to be said that the Fourier transform of such discontinuous functions certainly contains artifacts or spurious signals and therefore can only give a

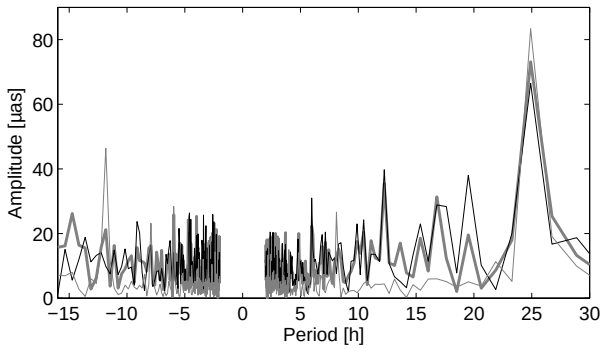

Figure 6: Amplitude spectrum of polar motion for CONT08 based on VLBI (*grey bold line*: Calc/Solve, *black line*: VieVS) and GPS (*grey thin line*) observations. Ocean tidal effects have been removed by applying the IERS Conventions model (McCarthy and Petit, 2004).

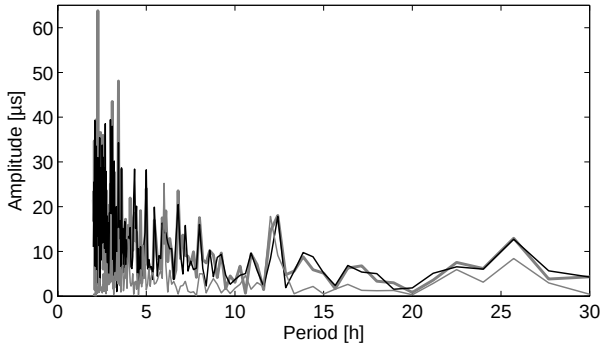

Figure 7: Amplitude spectrum of LOD for CONT08 based on VLBI (*grey bold line*: Calc/Solve, *black line*: VieVS) and GPS (*grey thin line*) observations. Ocean tidal effects have been removed by applying the IERS Conventions model (McCarthy and Petit, 2004).

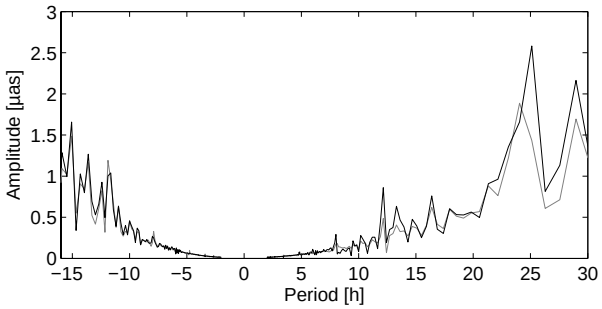

Figure 8: Amplitude spectrum of polar motion calculated from hourly AAM functions. *Black line*: concatenation variant 1, *grey line*: concatenation variant 2.

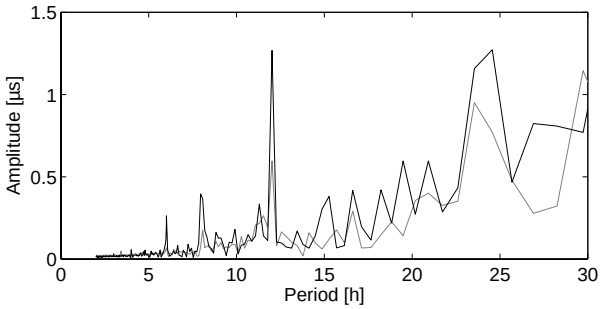

Figure 9: Amplitude spectrum of high-frequency LOD from hourly AAM functions. *Black line*: concatenation variant 1, *grey line*: concatenation variant 2.

rough measure of the sizes of amplitudes. However, we include this information in Table 1 (fifth data line). With the exception of the retrograde semi-diurnal band, the amplitudes generally remain small and thus clearly imply that the concatenation, even if it obviously smoothes the AAM values, does not account for the difference between hourly and six-hourly amplitude estimates.

Generally, the time span observed may be too short for deducing meaningful results about these discrepancies. Nonetheless, when examining in detail the amplitude spectra of the original and concatenated hourly AAM functions, an interesting feature can be detected: As indicated in Equations (7) and (12), matter and motion terms are always convolved with their corresponding transfer functions and subsequently added in frequency domain. This summation is performed separately for real and imaginary parts, and for χ_3 it reads

$$\Re\left(\chi_3\right) = \Re\left(\chi_3^p\right) + \Re\left(\chi_3^w\right), \tag{13}$$

$$\Im\left(\chi_3\right) = \Im\left(\chi_3^p\right) + \Im\left(\chi_3^w\right). \tag{14}$$

In the course of the addition, pressure and wind terms are likely to cancel out each other. Figure 10 illustrates this counteraction for the imaginary part of the equatorial component, which is particularly apparent for $T = +24$ h. Even in the time domain (Figure 11) the diurnal phase shift between χ_3^p and χ_3^w is clearly visible.

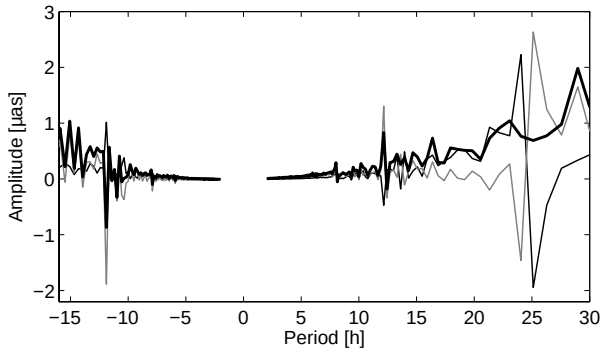

Figure 10: Imaginary part of the Fourier transform of polar motion from concatenated hourly AAM functions. *Black bold line*: matter plus motion terms, *black thin line*: matter term, *grey line*: motion term. Scale factor from the corresponding amplitude spectrum has been applied.

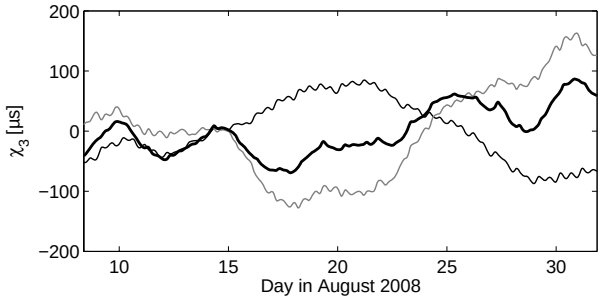

Figure 11: Concatenated hourly axial AAM function. *Black bold line*: matter plus motion terms, *black thin line*: matter term, *grey line*: motion term.

The observed anticorrelation of mass and motion terms can be ascribed to the relation of wind circulation and pressure distribution. Pressure gradient force is the main force that generates motion, acting to reduce the pressure gradient, or, in other words, prompting air to flow against the gradient and to reduce its potential energy to a lower geopotential. In the zonal case for example, consider a high pressure south of a low pressure in the northern hemisphere. This configuration causes wind to blow from south to north, which is then deflected by the Coriolis force to become a westerly wind, blowing from west to east. When this wind is strengthening, the motion term of the AAM is increasing, while the pressure gradient force is weakening, causing the mass portion of the AAM to reduce. Note however, that this process does not have an impact on the rotation of the solid Earth, as angular momentum is exchanged within the atmosphere only.

6 Conclusions and outlook

The basic concept of the angular momentum approach for studying high-frequency variations of Earth rotation has been reviewed. Comparison of ERP and high-resolution AAM functions is simple for the axial component, but otherwise involves transfer functions which take into account the Chandler frequency as well as the FCN resonance. Additionally, a special set of prefactors has to be used in order to consistently correct AAM functions for rotational and loading deformation under the assumption of a fully decoupled core.
We have evaluated whether hourly AAM functions from the 4DVar analysis of the ECMWF are useable for geodetic purposes just in the same way as the six-hourly estimates are.

A certain obstacle is the nature of the 4DVar algorithm itself, as it introduces jump discontinuities at 9 and 21 UTC in the AAM functions. Two ways of concatenating these 12 hour arcs have been found and applied, though others are possible. One has to keep in mind that spectral artifacts are present in the original discontinuous AAM as well as in the concatenated series due to the applied numerical scheme. Unless a rigorous procedure for handling the hourly AAM functions in frequency domain is employed, conclusions based on this dataset have to be treated with caution.

When estimating daily and sub-daily atmospheric excitation of polar motion and LOD for the year 2008, six-hourly AAM functions yield amplitudes close to the values found by Brzeziński and Petrov (2000). The atmospheric signals account only for about 25 % of the residual peaks in GPS-derived ERP, which were corrected for ocean tidal effects by means of the IERS Conventions model. Due to the inadequacy of the applied tidal model as well as the limited length of the investigated time series, the geodetic spectra still contain residual ocean tide signals. The size of these remainders can be several tens of μas, thus exceeding the atmospheric contribution to high-frequency variations of ERP and preventing thorough comparisons between geodetic data and atmospheric excitation. With hourly AAM functions for CONT08 based on the 4DVar analysis, the estimates from the six-hourly series cannot be reproduced. Both for the equatorial and axial component, pressure and wind terms seem to counteract each other, likely as a result of atmospheric circulation on short time scales, so that the amplitudes at diurnal and semi-diurnal frequencies become small. To confirm this result, however, it would be necessary to process 4DVar-based AAM functions for a longer time span than the three weeks investigated in this paper. Moreover, meteorological data from operational analysis with resolution higher than six hours would allow to validate our findings for hourly as well as six-hourly AAM functions.

Acknowledgements

This work was supported by project P20902-N10 of the Austrian Science Fund (FWF). The collaboration with co-author David Salstein was carried out within project SPEED

funded by the German Research Foundation (DFG). David Salstein is supported in part by Grant ATM-091370 from the U.S. National Science Foundation (NSF). We acknowledge the use of meteorological data of the ECMWF as well as the use of observations of the IVS and the IGS. We are grateful for the huge efforts of the staff at the IVS observatories participating in the CONT08 campaign and thank Thomas Artz (University of Bonn) and Peter Steigenberger (Technical University Munich) for providing the VLBI and GPS solutions. The valuable recommendations of three anonymous reviewers are also highly acknowledged.

References

1. Artz T., Böckmann S., Nothnagel A., Steigenberger P. Sub-diurnal variations in the Earth's rotation from continuous Very Long Baseline Interferometry campaigns, *J. Geophys. Res.*, 115, B05404, doi: 10.1029/2009JB006834, 2010.

2. Barnes R., Hide R., White A., Wilson C. Atmospheric angular momentum fluctuations, length-of-day changes and polar motion. *Proc. R. Soc. Lond*, A 387:31-73, 1983.

3. Bizouard C., Brzeziński A., Petrov S. Diurnal atmospheric forcing and temporal variations of the nutation amplitudes. *J. Geod.*, 72:561-577, 1998.

4. Böhm J., Spicakova H., Plank L., Teke K., Pany A., Wresnik J., Englich S., Nilsson T., Schuh H., Hobiger T., Ichikawa R., Koyama Y., Gotoh T., Kubooka T., Otsubo T. Plans for the Vienna VLBI Software VieVS. In Bourda G., Charlot P., Collioud A. (eds.), *Proceedings of the 19th European VLBI for Geodesy and Astrometry Working Meeting*, pages 161-164, 2009.

5. Brzeziński A. Polar motion excitation by variations of the effective angular momentum function, II: Extended model. *Manuscripta Geodaetica*, 19:157-171, 1994.

6. Brzeziński A., Bizouard C., Petrov S.D. Influence of the atmosphere on Earth rotation: What new can be learned from the recent atmospheric angular momentum estimates? *Surveys in Geophysics*, 23:33-69, 2002.

7. Brzeziński A., Petrov S. High frequency atmospheric excitation of Earth rotation. *IERS Technical Note*, 28:53-60, 2000.

8. Chao B., Ray R., Gipson J., Egbert G., Ma C. Diurnal/semidiurnal polar motion excited by oceanic tidal angular momentum. *J. Geophys. Res.*, 101(B9): 20151-20163, 1996.

9. Dickman S.R. Evaluation of "effective angular momentum function" formulations with respect to core-mantle coupling. *J. Geophys. Res.*, 108(B3), 2150, doi:10.1029/2001JB001603, 2003.

10. Dickman S.R. Rotationally consistent Love numbers. *Geophys. J. Int.*, 161: 31-40, 2005.

11. Eubanks T.M. Variations in the orientation of the Earth. In Smith D., Turcotte D. (eds.), *Contributions of Space Geodesy to Geodynamics: Earth Dynamics Geodynamics*, Volume 24, pages 1-54, American Geophysical Union, 1993.

12. Gordon D., MacMillan D., Baver K. Calc 10 implementation. In Behrend D., Baver K. (eds.), *International VLBI Service for Geodesy and Astrometry 2006 General Meeting Proceedings*, pages 291-295, 2006.

13. Gross R.S. Earth rotation variations - long period. In Herring T.A. (ed.), *Treatise on Geophysics*, Volume 3, Geodesy, pages 239-294. Elsevier, 2007.

14. Haas R. and Wünsch J. Sub-diurnal Earth rotation variations from the VLBI CONT02 campaign. *J. Geodyn.*, 41:94-99, doi: 10.1016/j.jog.2005.08.025, 2006.

15. Mathews P.M., Herring T.A., Buffett B.A. Modeling of nutation and precession: New nutation series for nonrigid Earth and insights into the Earth's interior. *J. Geophys. Res.*, 107(B4), 2068, doi:10.1029/2001JB000390, 2002.

16. McCarthy D.D. and Petit G. IERS Conventions 2003. *IERS Technical Note No. 32*, Verlag des Bundesamtes für Kartographie und Geodäsie, Frankfurt am Main, 2004.

17. Moritz H. and Mueller I.I. *Earth Rotation: Theory and Observation.* Ungar, New York, 1987.

18. Munk W.H., MacDonald G.J.F. *The Rotation of the Earth. A Geophysical Discussion.* Cambridge University Press, New York, 1960.

19. Perrson A., Grazzini F. User guide to ECMWF forecast products. http://ecmwf.int/products/forecasts/guide/, as at March 2007.

20. Ray R.D., Steinberg D.J., Chao B.F., Cartwright D.E. Diurnal and semidiurnal variations in the Earth's rotation rate induced by oceanic tides. *Science*, 264(5160): 830832, doi:10.1126/science.264.5160.830, 1994.

21. Sasao T. and Wahr J.M. An excitation mechanism for the free 'core nutation'. *Geophys. J. R. astr. Soc.*, 64: 729-746, 1981.

22. Salstein D.A., Kann D.M., Miller A.J., Rosen R.D. The sub-bureau for atmospheric angular momentum of the International Earth Rotation Service: A meteorological data center with geodetic applications. *Bulletin American Meteorological Society*, 74:67-80, 1993.

23. Steigenberger P., Rothacher M., Dietrich R., Fritsche M., Rülke A. Vey S. Reprocessing of a global GPS network. *J. Geophys. Res.*, 111, B05402, doi:10.1029/2005JB003747, 2006.

24. Vondrák J. and Ron C. Quasi-diurnal atmospheric and oceanic excitation of nutation. *Acta Geodyn. Geomater.*, 148: 121-128, 2007.

25. Wahr J.M. The effects of the atmosphere and oceans on the Earth's wobble - I. Theory. *Geophys. J. R. astr. Soc.*, 70: 349-372, 1982.

26. Wahr J.M. Polar motion models: Angular momentum approach. In Plag H.P., Chao B.F., Gross R.S., van Dam T. (eds.), *Forcing of Polar Motion in the Chandler Frequency Band: A Contribution to Understanding Interannual Climage Change.* Cahiers du Centre Européen de Géodynamique et du Séismologie, 24:1-7, Luxembourg, 2005.

27. Zharov V.E. and Gambis D. Atmospheric tides and rotation of the Earth. *J. Geod.*, 70:321-326, 1996.